Retrogressive thaw slump activity in the western Canadian Arctic (1984-2016)

Antoni G. Lewkowicz

Department of Geography, Environment and Geomatics – University of Ottawa, Ottawa, Ontario, Canada; alewkowi@uottawa.ca

This manuscript has been submitted for publication in Proceedings of the 12th International Conference on Permafrost in June 2024. It has undergone one round of peer-review but the manuscript has not yet been formally accepted for publication. Subsequent versions of this manuscript may have slightly different content. If accepted, the final version of this manuscript will be available via the “Peer-reviewed Publication DOI’ link on the right-hand side of this web-page. Please feel free to contact the author; feedback is welcomed.

Abstract

The spatial distribution and links to climate of retrogressive thaw slump (RTS) activity over 32 years were examined using Google Earth Engine Timelapse videos for five areas in the western Canadian Arctic totalling 150 000 km^2, each previously identified as having a high spatial concentration of these thermokarst landforms. Four spatial datasets run from 1984 to 2016 (Banks Island, northwest Victoria Island, Bluenose moraine, Paulatuk region), while the fifth starts in 2001 (Richardson Mountains / Peel Plateau). The total number of RTS active in the first four areas increased more than 50-fold, from 115 in 1984 to nearly 6000 in 2013. A further 573 RTS were active in this peak year in the Richardson Mountains / Peel Plateau. RTS developed most frequently adjacent to rivers (45%), with fewer on slopes (27%) or next to lakes (23%), and the smallest group at the coast (5%). However, there was considerable variation among the areas, and more than half in the Bluenose moraine and the Paulatuk region were initiated on lakeshores. High RTS initiations were linked to particularly warm summers, but once initiated, more than half of those RTS with long records remained active for more than 25 years. The impacts of this geomorphic activity included changes of colour in more than 500 lakes due to direct or indirect sediment inputs from RTS. The results show that the non-linear orders of magnitude increase from the 1980s to the 2010s previously reported for Banks Island extended across other ice-rich parts of the western Canadian Arctic.

1 Introduction

Retrogressive thaw slumps (RTS; Figure 1) are progressively expanding thermokarst landforms that develop from the subaerial exposure of near-surface ground ice and its subsequent melt over years to decades (Burn and Lewkowicz 1990). RTS have typical dimensions of tens to hundreds of metres and areas of a few hectares, but some grow sufficiently large that they have been termed megaslumps (e.g., Kokelj et al. 2015, 2023, Kizyakov et al. 2023). RTS formation requires high ice content sediments or massive ice near the top of permafrost, a triggering mechanism to expose the ice-rich substrate, and a slope sufficient to permit thawed soils to slide or flow away from the icy headscarp, maintaining its exposure. Once initiated, energy to melt the ice is mainly supplied in summer by solar radiation and sensible heat transfer from the air (Lewkowicz 1986, 1988). RTS stabilize in autumn as positive melt fluxes cease and the ground freezes. They restart the following summer providing the high ice-content layer and ground slope are not exhausted. Polycyclic RTS are common because a single transgression of an RTS headwall may not melt all the ground ice available (Mackay 1966, Lewkowicz 1987). Rainfall events, while not representing large heat fluxes, can re-mobilize debris in the floor of an RTS and expose this ice, resulting in renewed or enhanced activity (e.g., Kokelj et al. 2015).

RTS are highly concentrated spatially, being relatively uncommon across much of the Arctic (Nitze et al. 2018), while numbering in the hundreds or thousands in particularly ice-rich parts of the permafrost region (e.g., Jones et al. 2019, Lewkowicz and Way 2019, Kokelj et al. 2023, Yang et al. 2023). The latter include locations near the last glacial limit (Lacelle et al. 2015), areas that experienced still-stands during ice sheet recession (e.g., Kokelj et al. 2017, Nitze et al. 2021), and locations with thick ice-rich syngenetic permafrost (e.g., Zwieback et al. 2018). Within hillslope thermokarst landscapes (Olefeldt et al. 2016), RTS are initiated (1) at coasts, (2) on lakeshores, (3) on riverbanks, and (4) on slopes, disconnected from coasts, lakes or rivers, including in the floors of stabilized RTS. Until recently, it was generally assumed that RTS initiation related to waves and currents undercutting banks in the first three cases, and to thaw consolidation associated with active layer detachment formation in the fourth case. However, the strong temporal signal in initiation rates evident on Banks Island suggests that the thaw consolidation mechanism may apply to all four loci (Lewkowicz and Way 2019).

Figure 1. Example of an active RTS, Aulavik National Park, northern Banks Island, July 2019.

In this paper, datasets and analyses of RTS activity in four parts of the western Canadian Arctic are compared to those previously undertaken for Banks Island (Lewkowicz and Way 2019). The goals are to examine which of the latter's results pertain more widely. These include the increase in numbers of active RTS and their initiation relative to climate indices, the relative importance of the four loci of initiation, RTS longevity, and the number of lakes impacted. The research complements recent work that visually interpreted satellite images to map spatial concentrations of RTS and other thermokarst features in the NWT (Kokelj et al. 2023) and studies that employed machine-learning techniques to identify and delimit RTS extent in this and other parts of the permafrost region (e.g., Huang et al. 2020, Nitze et al. 2021, Lin and Knudby 2023, Yang et al. 2023).

2 Study Areas

The four new study areas (Table 1; northwest Victoria Island (VI), Bluenose moraine (BM), Paulatuk region (PR), and the Richardson Mountains/Peel Plateau (RM/PP)) are characterized by high or very high ice-content permafrost (O'Neill et al. 2019, 2022) and significant concentrations of RTS (Lacelle et al. 2015, Kokelj et al. 2017, 2023). Together with Banks Island (BI), they extend from 67.0°N to 74.6°N (Figure 2) and all are underlain by continuous permafrost, except for the easternmost portion of RM/PP which falls into the extensive discontinuous permafrost zone due to the abundance of surface water bodies (Heginbottom et al. 1995).

Mean annual air temperatures at proximal government weather stations range from -7°C to -13°C and July temperatures from 15°C to 7°C (1981-2010; Table 1). Mean annual precipitation follows a south to north gradient, ranging from 298 mm to 152 mm with more than half falling as snow. The BI, VI, and BM study areas have vegetation covers dominated by graminoid and prostrate-shrub tundras (CAVM Team 2003). The PR and RM/PP study areas extend across treeline with the latter's vegetation pattern being affected by elevation as well as latitude.

Table 1. Study areas in the western Canadian Arctic.

Study area[a]	Area (10^3 km^2)	Latitude (°N) and longitude (°W) ranges	Mean annual / mean July air temp. (°C)[b]	Period of analysis
BI	70	71.07–74.56; E. coast to W. coast	-12.8 / 6.6	1984-2016
VI	31	71.00–73.38; 113.90 to W. coast	-11.6 / 9.0	1984-2016
BM	21	67.75–69.77; 118.45–121.40	-10.3 / 10.9	1984-2016
PR	18	68.50–70.20; 122.70–125.43	-10.1 / 11.0	1984-2016
RM/PP	14	66.95–68.55; 134.85–136.75	-7.3 / 15.2	2001-2016

[a]BI: Banks Island; VI: NW Victoria Island; PR: Paulatuk region; BM: Bluenose moraine; RM/PP: Richardson Mountains / Peel Plateau. [b]At nearest station with 30-year climate normal (1981-2010): BI: Sachs Harbour; VI: Ulukhaktok; BM: Kugluktuk; PR: Tuktoyaktuk; RM/PP: Fort McPherson. Data from ECCC (2023a).

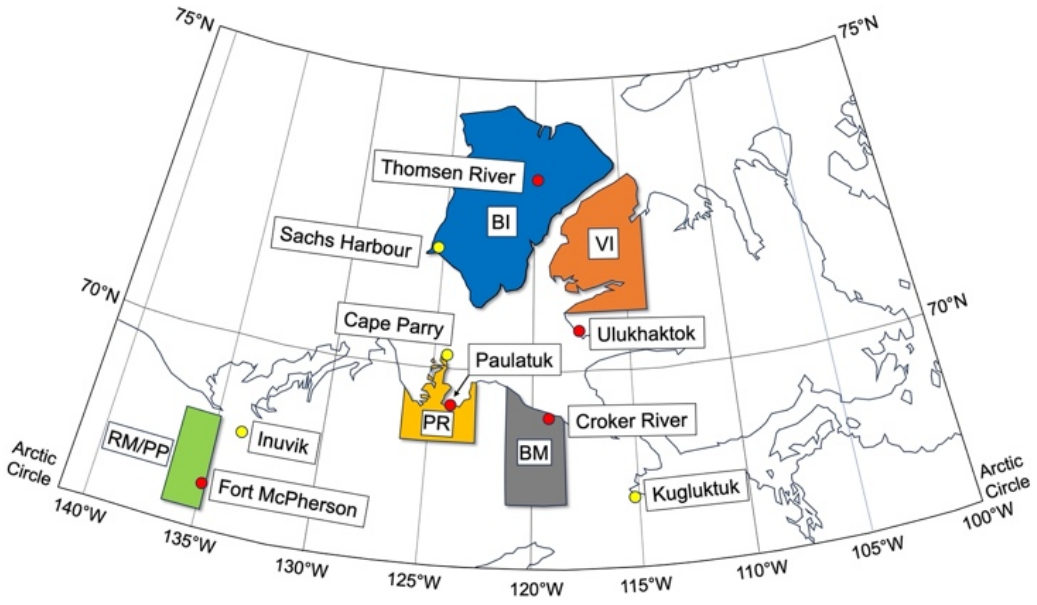

Figure 2. Study areas (see Table 1) and climate stations in the western Canadian Arctic. Study area colours correspond to those used in the line graphs (below). Red markers: representative climate stations for the study areas for the period of analysis. Yellow markers: stations used to infill missing data. Note: Sachs Harbour data were used to infill both Thomsen River and Ulukhaktok records.

3 Methods

RTS numbers, activity and locus of initiation, were analyzed using Google Earth Engine Timelapse, an internet-accessible resource that shows earth surface changes from satellite images assembled as a time-lapse video (Google Earth Engine 2023). Each frame of the video is cloud-free and shows a single year from 1984 onwards. The videos are mainly developed from Landsat data and have comparable resolutions (typically 30 m x 30 m) throughout the study period (see Lewkowicz and Way 2019). An active RTS can be detected visually (i.e., manually) because its headwall and adjacent saturated slump floor appear to move in the video as retrogression

takes place. Its location can then be recorded on a Google Earth image as a point, representing the approximate centroid of the slump (Lewkowicz and Way 2019). The year of initiation, the location of initiation in the landscape and the year of stability (if an RTS becomes inactive) can also be assessed by undertaking a frame-by-frame analysis. While this provides an annually resolved dataset, the first frame in which an RTS is visible is typically from the year following initiation because most RTS are either too small to be resolved in the satellite imagery in the year that they start or because the imagery from that year pre-dates RTS formation (Lewkowicz and Way 2019). Consequently, the initiation year recorded is often (but not always) lagged relative to the true date. It can also be challenging to precisely determine the year in which an RTS ceases to be active as stabilization typically manifests as a progressive reduction in the width of the active headwall and a gradual slowing of headwall retreat, rather than a sudden and definitive cessation of retrogression.

A small number of RTS which had been missed in the previously published analyses for BI (Lewkowicz and Way 2019) were added to that area's dataset for the time periods of 1984-2016 for total numbers and 1985-2015 for initiations. Data for the other study areas are analysed for the same periods, except for RM/PP where the record is shorter because images prior to 2001 are not included in the Google Earth Engine Timelapse imagery for this area (Table 1).

The previous inventory of RTS on BI was assessed as having errors of omission of 8% and of commission (incorrect identification of features as RTS) of 1% (Lewkowicz and Way 2019). More recently, mapping undertaken with high-resolution satellite images gave an overall agreement of 84% with the BI inventory (Kokelj et al. 2023). Errors in the current work should be comparable to those in Lewkowicz and Way (2019) except perhaps in some parts of the region where the imagery was of lower quality. The complete dataset will be made publicly available (Lewkowicz, in preparation). An example of the results is shown in Figure 3.

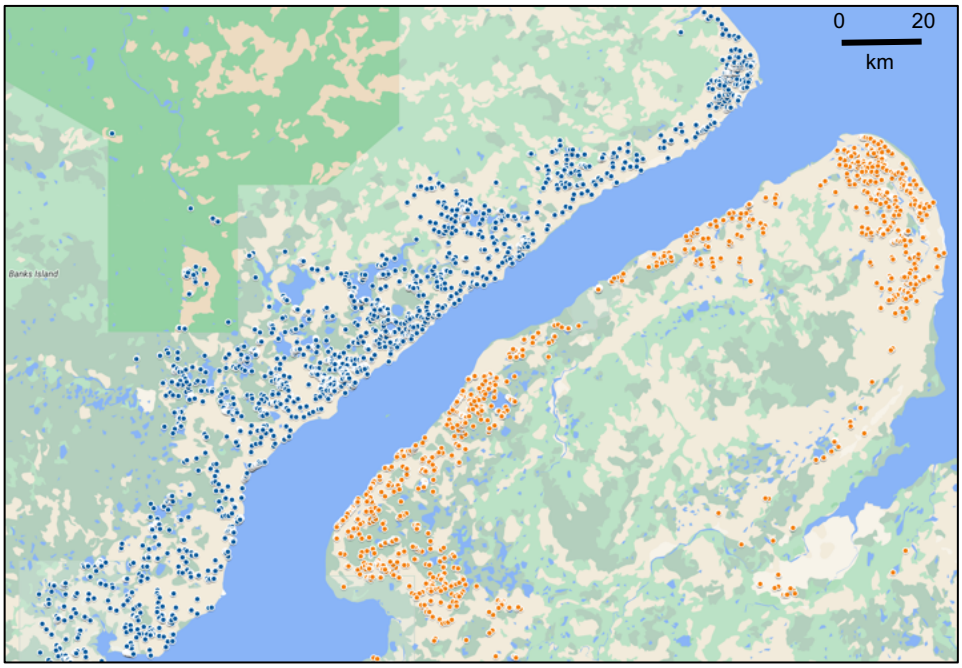

Figure 3. Locations of individual RTS active between 1984-2016 in the NE part of BI (blue markers, left) and the NW part of VI (orange markers, right). Base map source: Google Maps.

The duration of individual RTS activity was calculated from the dates assigned to the features during the inventorying process. This analysis took into account that the potential years of activity diminished through the record so that the longevity of some RTS could not be determined beyond a minimum number of years (Lewkowicz and Way 2019). Longevity rates were not calculated once the available sample size fell below 1% of the total number of RTS active in each study area.

Many lakes affected by sediment inputs from RTS changed colour in the Timelapse videos from dark blue to turquoise, or to beige. This reaction differs from some lakes in the Mackenzie Delta region which become clearer

due to RTS activity on their shorelines (Kokelj et al. 2009). The timing and duration of this qualitative change was recorded. Only lakes with a direct connection to active RTS (i.e., RTS present on the lakeshore) or an obvious indirect connection (RTS active upstream around a lake or on a valley floor) were included in the dataset. Some lakes exhibited up to three periods of changed colour, alternating with colour reversals. As with RTS activity, the potential duration of lake colour change diminished through the record and calculations took this into account. Given the much smaller number of lake colour changes compared to active RTS, a minimum sample size of 20% of the total number of lake colour changes in an area was required for the calculation to be undertaken.

Average summer (June to August) air temperatures for the study areas were compared to RTS initiation. The focus was on air temperature because precipitation was not revealed to be independently important in previous analyses for Banks Island (Lewkowicz and Way 2019). The air temperatures were extracted from the homogenized surface air temperature dataset (Vincent et al. 2020; Environment and Climate Change Canada 2023b) for the closest station (Figure 2). Gaps in the temporal records were infilled by regression based on highly correlated data (minimum r of 0.9) from nearby stations, where these were available for the missing years (Figure 2).

4. Results

Most results presented are for the four areas with datasets in common starting in 1984 and ending in 2016. Those from the RM/PP are included where possible.

4.1 Numbers of active RTS

More than 7400 individual RTS were active in the five study areas at some point during the record. The number of active RTS was consistently greatest on BI, with 50% or more of the total in every year, followed by VI, BM and PR (Figure 4). Numbers in RM/PP exceeded those in BM and PR after its record began in 2001.

The total number of active RTS for all four areas increased more than 50 times, from 115 active in 1984 to nearly 6000 in 2013. In VI, BM and PR, the number of active RTS increased by 71, 13 and 21 times, respectively, demonstrating that the orders of magnitude increase (64 times) previously reported for BI (Lewkowicz and Way 2019) was not confined to that island. A further 573 RTS were active in the RM/PP area in 2013 bringing the total in this peak activity year, to more than 6500. A slight decline then occurred as some RTS ceased activity and only a small number of RTS were newly initiated.

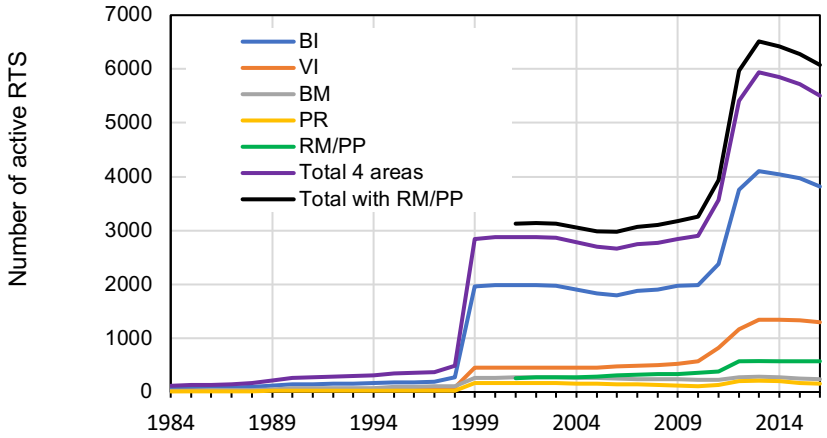

Figure 4. Number of active RTS in the study areas (1984-2016). BI: Banks Island; VI: Victoria Island; BM: Bluenose moraine; PR: Paulatuk region; RM/PP: Richardson Mountains / Peel Plateau (from 2001 onwards).

4.2 Location of RTS initiation

RTS within the study areas were highly concentrated spatially (e.g., see Figure 3). At the site level, the location of RTS initiation for the study areas combined was most frequently adjacent to rivers (45%), followed by slopes (27%), lakeshores (23%) and coasts (5%) (Table 2). BI and VI exhibit distributions in the landscape that are quite similar to the averages and to each other. In contrast, more than half of the RTS in BM and PR started along lake shorelines, there were fewer RTS on riverbanks and slopes, and virtually none on the coast. In RM/PP, two-thirds of the RTS initiated along rivers with almost all the remainder on slopes.

Table 2. Number and location of RTS initiation (1985-2015).

Study area	Number of RTS	Coast (%)	Lakeshore (%)	Riverbank (%)	Slope (%)
BI	4604	6.4	21.0	46.2	26.4
VI	1403	6.6	15.0	44.9	33.6
BM	440	0.0	55.3	35.8	8.9
PR	327	0.3	75.2	8.9	15.6
RM/PP[a]	632	-[b]	4.1	66.4	29.4
All areas	7406	5.2	22.8	45.4	26.5

[a] 2001-2015; [b] Study area does not include coastline.

4.3 Temporal variation in RTS initiation

RTS initiation was highly concentrated in the same small number of years in three of the four regions with a full record (Figure 5). More than 82% of all newly initiated RTS on VI and almost 79% in PR were first observed in just four of the 31 years: 1999, 2011, 2012 and 2013. These values are very similar to the 85% reported previously for BI for the same years (Lewkowicz and Way 2019). In BM, however, the percentage of the total initiated in the same years was only 56% and 2011 was not one of the top four initiation years. The truncated record for RM/PP means that fully comparable figures cannot be generated. However, visual observations of the size and rate of expansion of all RTS active at the start of the area's record in 2001 allowed an appraisal of whether they might have been first observable in 1999. Of the 256 RTS active in 2001, 45% were assessed as likely to have started two years earlier. When this figure is included in the newly initiated RTS number, the dominance of 1999 and 2012 also emerges for RM/PP (Figure 5).

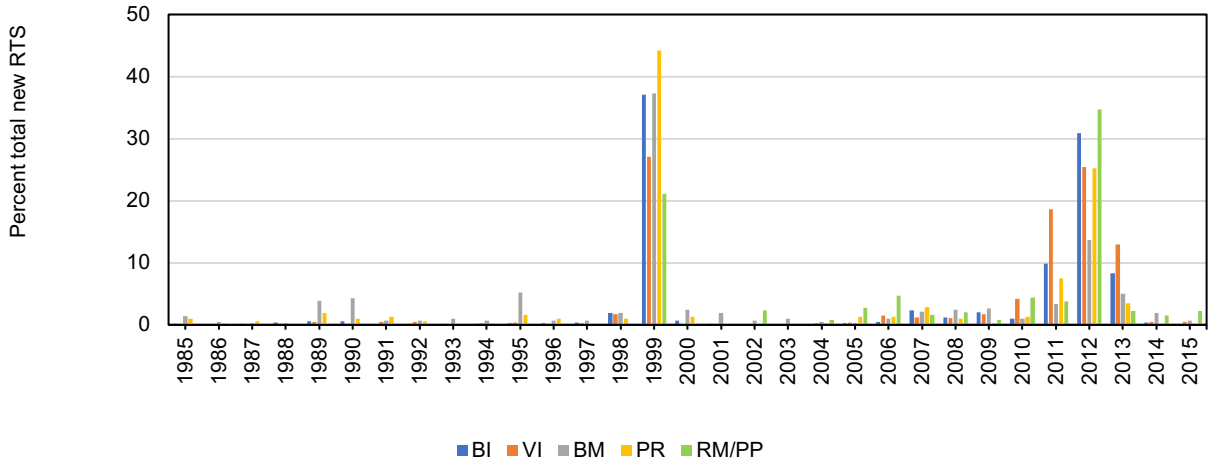

Figure 5. Temporal record of RTS initiation in the study areas (1985-2015). Note: for RM/PP, the record begins in 2002 but percentages include the 116 RTS active in 2001 that probably would have been observable in 1999 (see text); the column for 1999 is therefore an estimate.

4.4 Duration of RTS activity

Almost all the RTS identified were active for at least three years (Figure 6). This may partly reflect the methodology which likely would not have detected features active for shorter periods. The average probability of an RTS remaining active, based on all the data, gradually declined, reaching 55% after 25 years. The rate of decline, however, varied considerably: VI had the lowest rate, followed by BI, BM and PR. The last two reached 0% probability of an RTS remaining active after 30 years, while in VI, more than 80% were still active after 25

years. The truncated record for RM/PP lies between VI and BI but its slope was steeper for the last few points indicating that a greater percentage of RTS were beginning to stabilize (Figure 6).

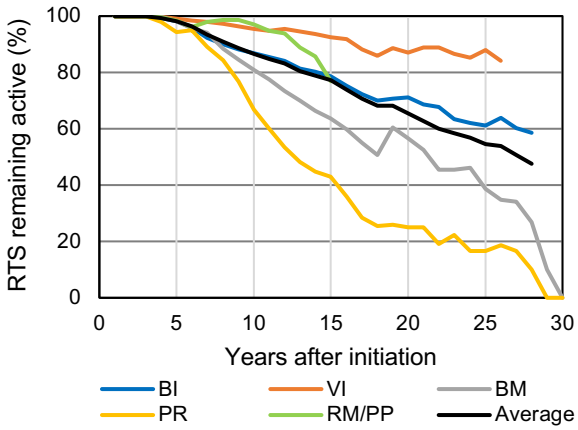

Figure 6. Duration of RTS activity. Note: lines are shown only for years when the sample size available exceeded 1% of the total number of RTS initiated in an area.

4.5 Impact of RTS on lake colour

Colour change due to RTS activity was observed in 574 individual lakes in the first four regions between 1984 and 2016. This number is substantial but it represents only a small fraction of the thousands of ponds and lakes in the study regions. Half of the lakes affected (288) were on BI with most of the rest divided equally between VI (124) and BM (123) (Figure 7). PR had 39 lakes with changed colour. Only 11 were observed as being impacted in RM/PP after 2001, and given this small number and shorter record, these data were not analysed further.

At the start of the record in 1984, 13 lakes in the first four regions were being affected by sediment inputs from RTS and almost all of these were in BM (Figure 8). Numbers grew during the 1990s but as with RTS initiation, the first major increase was observed in 1999 when 176 lakes changed colour and the total rose to 195. Other years when substantial numbers of lakes changed colour were 2007, 2012 and 2013. In between these years, some lakes experienced colour reversals resulting in slight declines in the total of those visibly affected (Figure 8). These reversals occurred mainly where RTS had stabilized, but at some sites, they were observed even though RTS headscarps continued to retreat. The latter is likely linked to decreases in exports of ground ice meltwater and its associated sediment load as the headwall retreated progressively from the lakeshore.

The average trend for the duration of lake colour change showed that about half of the lakes returned to their original colour within 15 years (Figure 9). The ordering among the study areas was similar to RTS longevity, with altered lake colour continuing longest for lakes in VI, while the shortest duration was in PR. However, BI and BM were similar which was not the case for RTS longevity (see Figure 6). The combination of relatively lengthy persistence for colour change and the number of newly affected lakes meant that the peak number of 429 was reached in 2013 (Figure 8), representing a 33-fold increase compared to 1984.

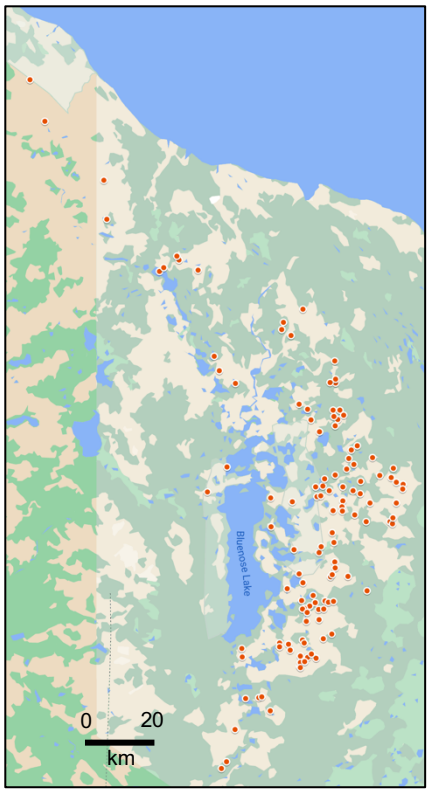

Figure 7. Spatial distribution of 124 lakes in BM that experienced colour change (red markers) due to RTS activity (1984-2016). Base map source: Google Maps.

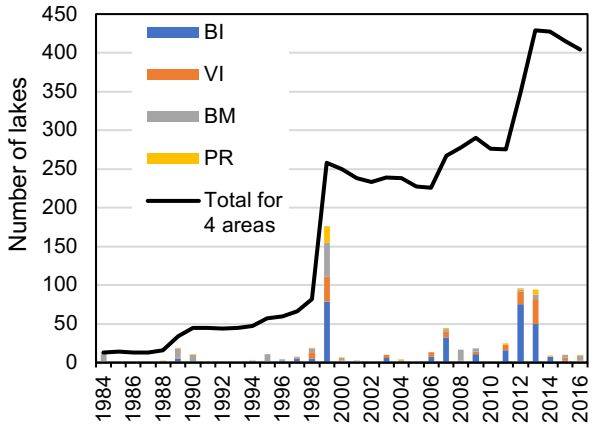

Figure 8. Number of lakes changing colour due to RTS activity (1984-2016). Stacked bars show new colour changes in the four areas with a complete record. Black line shows total number of lakes with changed colour for the same areas.

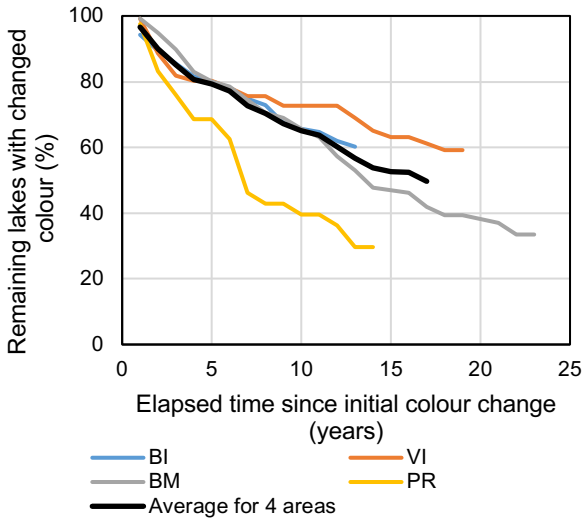

Figure 9. Duration of lake colour change for four study areas. Note: lines are shown only for the period when the remaining number of lakes exceeded 20% of the total initial number.

Rapid shoreline retreat forming a new bay was observed in a small number of lakes that also experienced colour change. Fourteen were affected in BM, four on BI, one on VI and one in PR, with shoreline retreat of up to 300 m over a decade. At these sites, the terrain slope is low enough and lakeside sediments are sufficiently ice-rich that their thaw results in land subsidence to below the elevation of the lake water. In each case, an RTS developed at the head of the new bay immediately following stabilization of the shoreline.

4.6 RTS initiation and summer climate

The relationship between RTS initiation and mean summer (June to August) air temperatures was examined for all five study areas. The air temperature used as the independent variable was that of the previous summer because of the expected lag in observation of initiation. Strong positive log-linear relationships were present for BI and BM (r^2 = 0.61 and 0.56, respectively), weaker relationships for VI and PR (r^2 = 0.36 and 0.30, respectively), and no relationship for the shorter record at RM/PP (r^2 = 0.03) (Figure 10). However, even though log-linear relationships were used, the best-fit lines substantially underestimated numbers of new RTS in the peak initiation years.

Summer air temperatures linked to high levels of RTS initiation were area-specific. The lowest values were at BI and the highest at RM/PP. This underlines that it is the climatic extremes in a given distribution, not absolute values, that trigger major initiation events.

Satellite image videos available on Google Earth Engine Timelapse now (in early 2024) run until 2022. However, the period of systematic analyses was not extended beyond that used for BI in Lewkowicz and Way (2019) due to the large amount of observer time that would have been required. Instead, a reconnaissance-level investigation of high concentration areas of RTS in each of the study areas was undertaken. This showed that many of the RTS initiated in 1998 or later remained active and continued to expand rapidly after 2016, but few newly-initiated RTS were observed. This tentative result fits with the record of mean summer air temperatures for 2017-2022 across the region, none of which exceeded those of 1998 and 2012.

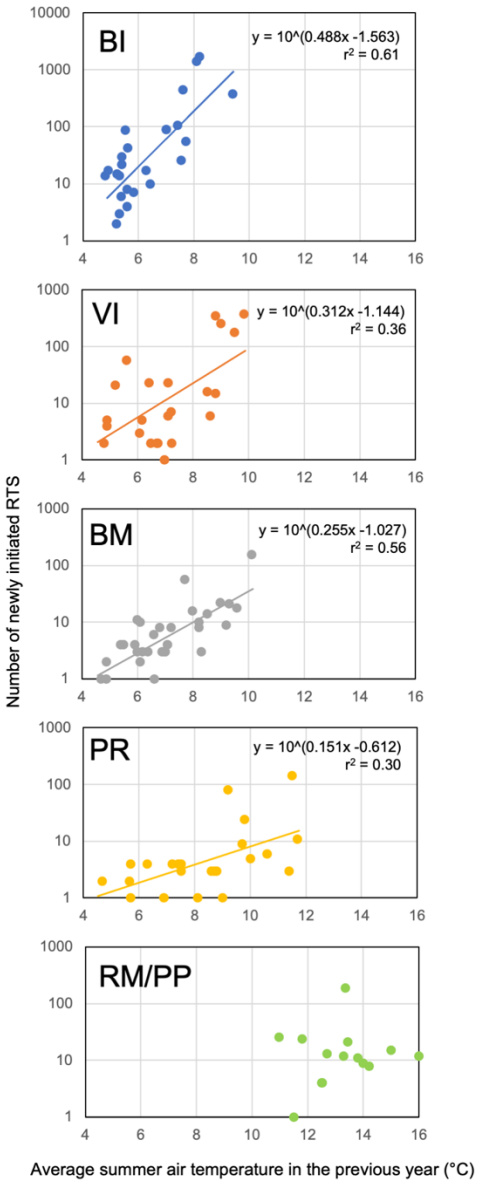

Figure 10. Relationship between average summer (June, July, August) air temperature in the previous year and the number of newly observed RTS in the five study areas. Note the logarithmic y-axis. Statistically significant log-linear relationships are shown. Years without newly observed RTS were excluded from the regression analyses.

5 Discussion and conclusions

The simple counts of RTS reported here are useful primarily to indicate the spatial distribution of these thermokarst features and to evaluate the links between temporal change and climate. The datasets can also be used to validate machine-learning methods related to RTS (e.g., Huang et al. 2023, Lin and Knudby 2023). They cannot be used to provide details on RTS area, ice volume loss, rate of headwall retreat or many other geomorphological characteristics. Development of such data requires different methodologies, such as UAV imaging (e.g., Armstrong et al. 2018, Van der Sluijs et al. 2018, Hayes et al. 2022), AI techniques (e.g., Huang et al. 2020, 2022, Nitze et al. 2021), or RTS demarcation using high resolution satellite images (e.g., Rudy et al. 2017).

Despite the information limits imposed by the methodology, some significant results emerge from this comparative study. They support conclusions previously reached for Banks Island (Lewkowicz and Way 2019) while enlarging the geographical context.

First, active RTS demonstrably proliferated in areas of ice-rich permafrost in the western Canadian Arctic, starting in the warm summer of 1998. Numbers rose 13 to 71 times from 1984 to 2016 in the four study areas with complete records (Banks Island, NW Victoria Island, Bluenose moraine, Paulatuk region). With the addition of the truncated record for the Richardson Mountains/Peel Plateau, more than 6500 RTS were active in the peak summer of 2013. Once started, more than half of the all the RTS remained active for more than two decades, although longevity varied among the study areas.

Second, the distribution of RTS across the landscape varied by study area, with lakeshore RTS being the most important numerically in BM and PR, and riverbank RTS being the most important in the other areas. These differences likely relate to physiography and the distribution of ground ice, but additional investigation is required to identify the critical variables.

Third, more than 500 lakes were impacted sufficiently by RTS activity to exhibit a change in colour that in turn relates to turbidity, with a peak of 429 affected lakes in 2013. Lake colour reversal took longest on Victoria Island, which was also the area where RTS were the longest-lasting.

Finally, the relationships between summer climate and RTS initiation show that it is exceedance of thaw probability for a particular area that matters, not the absolute value. Predictions of RTS initiation rates can be made using summer air temperature series, but even these log-linear relationships underestimate the number of newly initiated slumps in exceptional summers. This result underlines the threshold nature of initiation, likely linked to the thaw depths necessary to reach high ice content layers (such as buried ice). As a result, RTS activity can be expected to accelerate as the climate warms in future decades and extreme thaw events penetrate to still greater depths.

A cursory review of Timelapse videos for the study areas suggested that no major initiation events occurred from 2017-2022 and this aligns with an absence of high recurrence interval warm summers during this period. Until 2023, therefore, the summers of 2012/2013 appeared to be the latest episodes in which more than a thousand new RTS were initiated across the region. However, the impacts of those years and the earlier warm summer of 1998 continued to affect the landscape of the western Canadian Arctic as many RTS initiated then remained active. Furthermore, average air temperatures in the study areas in summer 2023 (data from ECCC 2023c) equalled or exceeded the values from 1998 and 2012. Time will tell whether this led to extensive RTS initiation but it seems likely given past relationships (Figure 10).

6 Acknowledgments

Students in the GEG 4101 Permafrost Environments class at the University of Ottawa in the 2019 winter semester are thanked for their initial review of RTS activity within the NW Victoria Island study area. Dr. Robert Way is thanked for his contribution to the previous publication that focused exclusively on Banks Island. The author is grateful to the two reviewers for helpful comments on an earlier version of the manuscript.

7 References

Armstrong, L., Lacelle, D., Fraser, R.H., Kokelj, S. and Knudby, A., 2018. Thaw slump activity measured using stationary cameras in time-lapse and Structure-from-Motion photogrammetry. Arctic Science, 4(4): 827-845.

Burn, C.R. and Lewkowicz, A.G. 1990. Canadian Landform Examples - 17: Retrogressive thaw slumps. The Canadian Geographer, 34(3): 273-276.

CAVM Team, 2003. Circumpolar Arctic Vegetation Map. Scale 1:7,500,000. Conservation of Arctic Flora and Fauna (CAFF) Map No. 1. U.S. Fish and Wildlife Service, Anchorage, Alaska.

Environment and Climate Change Canada. 2023a. Climate normals. https://climate.weather.gc.ca/climate_normals/ Accessed August 31, 2023.

Environment and Climate Change Canada. 2023b. Climate data: homogenized surface air temperature data. https://www.canada.ca/en/environment-climate-change/services/climate-change/science-research-data/climate-trends-variability/adjusted-homogenized-canadian-data/surface-air-temperature.html Accessed August 31, 2023.

Environment and Climate Change Canada. 2023c. Daily data report: Cape Parry, Croker River, Fort McPherson, Inuvik, Kugluktuk, Paulatuk, Sachs Harbour, Thomsen River, Ulukhaktok. https://climate.weather.gc.ca/historical_data/search_historic_data_stations_e.html Accessed November 15, 2023.

Google Earth Engine. 2023. Timelapse, https://earthengine.google.com/timelapse/ Accessed August 1, 2023.

Hayes, S., Lim, M., Whalen, D., Mann, P.J., Fraser, P., Penlington, R. and Martin, J. 2022. The role of massive ice and exposed headwall properties on retrogressive thaw slump activity. Journal of Geophysical Research: Earth Surface, 127(11): e2022JF006602.

Heginbottom, J.A., Dubreuil, M.-A., and Harker, P. 1995. Permafrost - Canada (National Atlas of Canada MCR 4177, scale 1:7,500,000). Energy, Mines, and Resources Canada.

Huang, L., Lantz, T.C., Fraser, R.H., Tiampo, K.F., Willis, M.J. and Schaefer, K., 2022. Accuracy, efficiency, and transferability of a deep learning model for mapping retrogressive thaw slumps across the Canadian Arctic. Remote Sensing, 14(12): 2747.

Huang, L., Luo, J., Lin, Z., Niu, F. and Liu, L. 2020. Using deep learning to map retrogressive thaw slumps in the Beiluhe region (Tibetan Plateau) from CubeSat images. Remote Sensing of Environment, 237: 111534.

Huang, L., Willis, M.J., Li, G., Lantz, T.C., Schaefer, K., Wig, E., Cao, G. and Tiampo, K.F., 2023. Identifying active retrogressive thaw slumps from ArcticDEM. ISPRS Journal of Photogrammetry and Remote Sensing, 205: 301-316.

Jones, M.K.W., Pollard, W.H. and Jones, B.M. 2019. Rapid initialization of retrogressive thaw slumps in the Canadian high Arctic and their response to climate and terrain factors. Environmental Research Letters, 14(5): 055006.

Kizyakov, A.I., Wetterich, S., Günther, F., Opel, T., Jongejans, L.L., Courtin, J., Meyer, H., Shepelev, A.G., Syromyatnikov, I.I., Fedorov, A.N. and Zimin, M.V. 2023. Landforms and degradation pattern of the Batagay thaw slump, Northeastern Siberia. Geomorphology, 420: 108501.

Kokelj, S.V., Gingras-Hill, T., Daly, S.V., Morse, P., Wolfe, S., Rudy, A.C., van der Sluijs, J., Weiss, N., O'Neill, B., Baltzer, J. and Lantz, T.C. 2023. The Northwest Territories Thermokarst Mapping Collective: A northern-driven mapping collaborative toward understanding the effects of permafrost thaw. Arctic Science, 9(4): 886-918.

Kokelj, S. V., Lantz, T. C., Tunnicliffe, J., Segal, R. and Lacelle, D. 2017. Climate-driven thaw of permafrost preserved glacial landscapes, northwestern Canada. Geology 45: 371–374.

Kokelj, S.V., Tunnicliffe, J., Lacelle, D., Lantz, T.C., Chin, K.S. and Fraser, R. 2015. Increased precipitation drives mega slump development and destabilization of ice-rich permafrost terrain, northwestern Canada. Global and Planetary Change, 129: 56-68.

Kokelj, S.V., Zajdlik, B. and Thompson, M.S. 2009. The impacts of thawing permafrost on the chemistry of lakes across the subarctic boreal-tundra transition, Mackenzie Delta region, Canada. Permafrost and Periglacial Processes, 20(2): 185-199.

Lacelle, D., Brooker, A., Fraser, R.H. and Kokelj, S.V. 2015. Distribution and growth of thaw slumps in the Richardson Mountains–Peel Plateau region, northwestern Canada. Geomorphology, 235: 40-51.

Lewkowicz, A.G. 1986. Rate of short-term ablation of exposed ground ice, Banks Island, Northwest Territories, Canada. Journal of Glaciology, 32(112): 511-519.

Lewkowicz, A.G. 1987. Nature and importance of thermokarst processes, Banks Island, Canada. Geografiska Annaler, 69A: 321-327.

Lewkowicz, A.G. 1988. Ablation of massive ground ice, Mackenzie Delta, In Proceedings, Fifth International Conference on Permafrost, Trondheim, August 1988, Trondheim, Tapir: 605-610.

Lewkowicz, A.G. and Way, R.G. 2019. Extremes of summer climate trigger thousands of thermokarst landslides in a High Arctic environment. Nature Communications, 10(1): 1329.

Lewkowicz, A.G. in preparation. Retrogressive thaw slump activity and related lake colour change in five areas of the western Canadian Arctic. Planned for submission to Nordicana D.

Lin, Y. and Knudby, A.J. 2023. A transfer learning approach for automatic mapping of retrogressive thaw slumps (RTS) in the western Canadian Arctic. International Journal of Remote Sensing, 44(6): 2039-2063.

Mackay, J.R. 1966. Segregated epigenetic ice and slumps in permafrost, Mackenzie Delta area, N.W.T.. Geographical Bulletin, 8: 59-80.

Nitze, I., Grosse, G., Jones, B.M., Romanovsky, V.E., and Boike, J. 2018. Remote sensing quantifies widespread abundance of permafrost region disturbances across the Arctic and Subarctic. Nature Communications, 9..

Nitze, I., Heidler, K., Barth, S. and Grosse, G. 2021. Developing and testing a deep learning approach for mapping retrogressive thaw slumps. Remote Sensing, 13(21): 4294.

Olefeldt, D., Goswami, S., Grosse, G., Hayes, D., Hugelius, G., Kuhry, P., Mcguire, A.D., Romanovsky, V.E., Sannel, A.B.K., Schuur, E.A.G., and Turetsky, M.R. 2016. Circumpolar distribution and carbon storage of thermokarst landscapes. Nature Communications 7.

O'Neill, H.B., Wolfe, S.A. and Duchesne, C., 2019. New ground ice maps for Canada using a paleogeographic modelling approach. The Cryosphere 13(3): 753-773.

O'Neill, H.B., Wolfe, S.A., Duchesne, C. 2022. Ground ice map of Canada v.1.1. Geological Survey of Canada Open File 8713.

Rudy, A.C.A., Lamoureux, S.F., Kokelj, S.V., Smith, I.R. and England, J.H. 2017. Accelerating thermokarst transforms ice-cored terrain triggering a downstream cascade to the ocean. Geophysical Research Letters, 44(21): 11-080.

Van der Sluijs, J., Kokelj, S.V., Fraser, R.H., Tunnicliffe, J. and Lacelle, D. 2018. Permafrost terrain dynamics and infrastructure impacts revealed by UAV photogrammetry and thermal imaging. Remote Sensing, 10(11): 1734.

Vincent, L. A., Hartwell, M.M. and Wang, X.L. 2020. A third generation of homogenized temperature for trend analysis and monitoring changes in Canada's climate. Atmosphere-Ocean, 58(3): 173-191.

Yang, D., Qiu, H., Ye, B., Liu, Y., Zhang, J. and Zhu, Y. 2023. Distribution and recurrence of warming-induced retrogressive thaw slumps on the Central Qinghai-Tibet Plateau. Journal of Geophysical Research: Earth Surface: e2022JF007047.

Zwieback, S., Kokelj, S.V., Günther, F., Boike, J., Grosse, G. and Hajnsek, I. 2018. Sub-seasonal thaw slump mass wasting is not consistently energy limited at the landscape scale. The Cryosphere, 12(2): 549-564.